Synthetic Zinc Finger Transcription Factor Action at an Endogenous Chromosomal Site

ACTIVATION OF THE HUMAN ERYTHROPOIETIN GENE*

Lei Zhang, S. Kaye Spratt, Qiang Liu, Brian Johnstone, Hong Qi, Eva E. Raschke, Andrew C. Jamieson, Edward J. Rebar, Alan P. Wolffe‡, and Casey C. Case

From Sangamo BioSciences Inc., Point Richmond Tech Center, Richmond, California 94804

We have targeted the activation of an endogenous chromosomal locus including the human erythropoietin gene using synthetic transcription factors. These transcription factors are targeted to particular DNA sequences in the 5'-flanking region of the erythropoietin gene through engineering of a zinc finger DNA binding domain. The DNA binding domain is linked to a VP16 transcriptional activation domain. We find that these synthetic transcription factors invariably activate transiently transfected templates in which sequences within the 5' flank of the erythropoietin gene are fused to a luciferase reporter. The efficiency of activation under these circumstances at a defined site is dependent on DNA binding affinity. In contrast, only a subset of these same zinc finger proteins is able to activate the endogenous chromosomal locus. The activity of these proteins is influenced by their capacity to gain access to their recognition elements within the chromatin infrastructure. Zinc finger transcription factors will provide a powerful tool to probe the determinants of chromatin accessibility and remodeling within endogenous chromosomal loci.

The enormous progress in our understanding of gene control in eukaryotes using model systems presents substantial opportunities to apply this knowledge for therapeutic benefit in man. The rational design and engineering of components of the transcriptional machinery provide a powerful means to test conventional paradigms for the roles of protein-DNA and protein-protein interactions in gene regulation. These designer transcription factors may also provide novel means of regulating endogenous chromosomal loci for a variety of beneficial purposes. Over the past decade, the primary structural determinants of DNA recognition by zinc fingers of the Cys_2-His_2 type have been elucidated (1–8). Designer transcriptional regulators containing three or more zinc finger domains have been used in isolation (9, 10) or following linkage to transcriptional activation (9, 11–13) or repression domains (12, 13). These novel proteins control the transcription of reporter genes both transiently transfected into human cells (9, 11–13) and endogenous chromosomal loci (9, 13). Exactly how these regulatory functions are exerted remains to be resolved. An important

issue in considering transcription factor function in eukaryotes is the capacity of the regulator to gain access to specific sites in chromatin and recruit transcriptional co-activators and co-repressors that modify the chromatin environment (14). These issues have been investigated for the archetypal Cys_2-His_2 zinc finger protein and transcriptional regulator TFIIIA[1] (15–26). There is general agreement that the nucleosome can impede recognition of specific promoter elements by TFIIIA (15, 17–26) and that modification of histone-DNA interactions through nucleosome repositioning (18, 19), histone depletion (20, 21), and removal of the histone tails (22, 23) can promote TFIIIA binding to a nucleosomal infrastructure. Accumulation of histone H1 in chromatin can specifically interfere with TFIIIA function *in vivo* (24, 25) in a process that involves the repositioning of nucleosomes (25, 26). These studies demonstrate the role of chromatin infrastructure access by transcription regulators containing zinc finger DNA binding domains of the Cys_2-His_2 type.

In this work, we first designed 10 novel zinc finger DNA binding domains to recognize specific 9-bp sequences in the 5' flank of the erythropoietin gene and characterized their unique DNA recognition selectivities and variable affinities for DNA. These zinc finger domains were then linked to the VP16 transcriptional activation domain (27) and tested for their capacity to activate transcription in both transient transfections and from endogenous chromosomal loci. Our results indicate that all of our synthetic regulators that bind DNA *in vitro* with dissociation constants <10 nM can activate transiently transfected templates. This activation of a particular site is dependent on DNA binding affinity. In contrast, only a subset of the synthetic regulators can activate the endogenous chromosomal locus.

We find that the regulators that work in the endogenous chromosome can bind within the chromatin infrastructure, but that the differential binding of distinct regulators at a particular site is largely independent of primary DNA binding affinity. These studies indicate that chromosome and chromatin organization is a determinant of zinc finger transcription factor function within endogenous chromosomal loci.
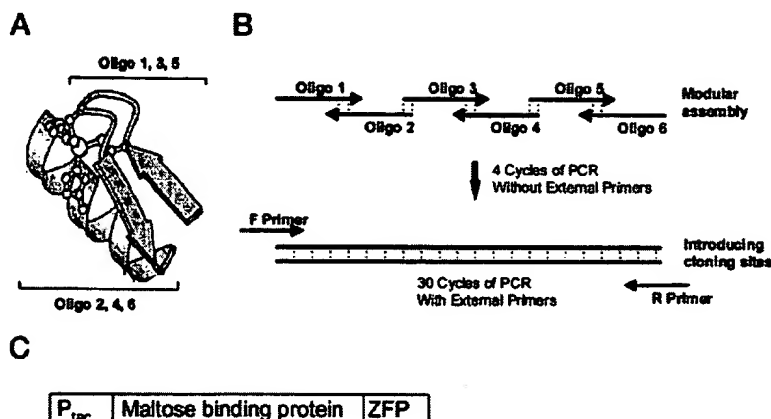
EXPERIMENTAL PROCEDURES

Design, Synthesis, and Purification of Zinc Finger Proteins—The foundation for our design strategy was to scan 1000 bp of the 5'-

[1] The abbreviations used are: TFIIIA, transcription factor IIIA; bp, base pair(s); PCR, polymerase chain reaction; oligo, oligonucleotide; CMV, cytomegalovirus; β-gal, β-galactosidase; PBS, phosphate-buffered saline; ZFP, zinc finger protein; EPO, erythropoietin; HEK, human embryonic kidney; Dox, doxycycline; ELISA, enzyme-linked immunosorbent assay; GAPDH, glyceraldehyde-3-phosphate dehydrogenase; EPOZFP, erythropoietin-directed zinc finger proteins.

FIG. 1. **The construction scheme of EPOZFPs.** *A*, the structure of an individual zinc finger with two β-sheets linked to the DNA-binding α- helix. Oligos 1, 3, and 5 comprise the β-sheet regions, and oligos 2, 4, and 6 comprise the DNA-binding α-helix regions. *B*, the assembly scheme of the ZFPs. Six overlapping oligonucleotides were annealed and amplified with a pair of external oligonucleotides. The PCR products were then cut with *Kpn*I and *Bam*HI, before cloning into the pMalC2 bacterial expression vector. *C*, scheme of the maltose-binding EPOZFP fusions.

TABLE I
The designs of the EPO-binding ZFPs

Name	Target sequence 5' → 3'	Subsites 5' → 3'	Designs −1 → +6
EPOZFP−862a	GCGGTGGCTc	F1GCTc	QSSDLQR
		F2GTGg	RSDALSR
		F3GCGg	RSDERKR
EPOZFP−862b	GCGGTGGCTc	F1GCTc	QSSDLQR
		F2GTGg	RSDALSR
		F3GCGg	RSDTLKK
EPOZFP−862c	GCGGTGGCTc	F1GCTc	QSSDLTR
		F2GTGg	RSDALSR
		F3GCGg	RSDERKR
EPOZFP−545a	GGTGAGGAGt	F1GAGt	RSDNLAR
		F2GAGg	RSDNLAR
		F3GGTg	DSSKLSR
EPOZFP−545b	GGTGAGGAGt	F1GAGt	RSDNLAR
		F2GAGg	RSDNLAR
		F3GGTg	MSDHLSR
EPOZFP−535	GAGGTGGGGa	F1GGGa	RSDHLAR
		F2GTGg	RSDALSR
		F3GAGg	RSDNLSR
EPOZFP−233	TGGGTCGCGg	F1GCGg	RADTLRR
		F2GTCg	DRSALAR
		F3TGGg	RSDHLTT
EPOZFP−82	GTGGGGGAGa	F1GAGa	RSDNLAR
		F2GGGg	RSDHLSR
		F3GTGg	RSDALAR
EPOZFP−72	GCGGGTGGGg	F1GGGg	RSDHLAR
		F2GGTg	QSSHLAR
		F3GCGg	RSDDLTR
Sp1	GGGGCGGGGt	F1GGGt	KTSHLRA
		F2GCGg	RSDELQR
		F3GGGg	RSDHLSK
Zif268	GCGTGGGCGt	F1GCGt	RSDELTR
		F2TGGg	RSDHLTT
		F3GCGt	RSDERKR

flanking sequences of the human erythropoietin (EPO) gene to choose the best candidate recognition elements for which to design zinc finger DNA binding domains. The human transcription factor Sp1 (amino acids 532–624) was used as the backbone to assemble 10 distinct zinc finger DNA binding domains. The design determinants of these proteins will be described elsewhere[2]; however, the amino acid sequences chosen to recognize particular sequences are illustrated in Table I. Our strategy to synthesize the zinc finger DNA binding domains is outlined in Fig. 1. To create the synthetic genes encoding EPO-directed zinc finger proteins (EPOZFPs), a polymerase chain reaction (PCR)-based assembly procedure was applied using six overlapping oligonucleotides. Three oligonucleotides for the zinc finger coding sequences encode portions of the DNA binding domain containing the β sheet and linker regions between the α-helical DNA recognition sequences of the Sp1 zinc finger DNA binding domain scaffold (Fig. 1A, oligos 1, 3, and 5). The other three oligonucleotides encode the recognition helices (oligos 2, 4, and 6). The overlap between adjacent oligonucleotides is 15 base pairs. The PCR synthesis was carried out in two steps (Fig. 1B). First, the double-stranded DNA template was created by combining the six oligos and filling the gaps with a four-cycle PCR reaction (using *Taq* and *Pfu* thermostable DNA polymerases). The annealing temperature was 25 °C, a temperature at which the six oligos would anneal to form a DNA scaffold. In the second phase of construction, the template was amplified using a pair or external primers containing *Kpn*I and *Bam*HI restriction sites. The PCR products were directly cloned into the Tac promoter vector, pMal-c2 (New England Biolabs, Beverly, MA), using *Kpn*I and *Bam*HI restriction sites. The zinc finger proteins were purified as fusions with the maltose-binding protein (Fig. 1C) according to the manufacturer's instructions (New England Biolabs, Beverly, MA). The purified ZFPs (see Fig. 2A) were tested for their affinities for the DNA recognition sites within the 5' flank of the EPO gene. DNA oligonucleotides 30 base pairs in length that contain the various sites were synthesized, annealed, and end-labeled using polynucleotide kinase and [γ-^{32}P]ATP. Binding of the ZFPs to target oligonucleotides was performed by titrating protein against a fixed amount of duplex substrate. Twenty-µl binding reactions contained 50 pM 5'-^{32}P-labeled double-stranded target DNA, 10 mM Tris-HCl (pH 7.5), 100 mM KCl, 1 mM MgCl$_2$, 1 mM dithiothreitol, 10% glycerol, 200 µg/ml bovine serum albumin, 0.02% Nonidet P-40, and 100 µM ZnCl$_2$. Binding was allowed to proceed for 45 min at room temperature. Polyacrylamide gel electrophoresis was carried out at room temperature using precast 10% or 10–20% Tris-HCl gels (Bio-Rad) and Tris-glycine running buffer (25 mM Tris-HCl, 192 mM glycine (pH 8.3)). The radioactive signals were quantitated with a PhosphorImager and autoradiographed. Once the DNA binding properties of the zinc finger DNA binding domains had been tested, these domains were subcloned into eukaryotic expression vectors. The vector used was generated based upon a ZFP-less expression vector pcDNA-NVF, which was modified from pcDNA3.1 (Invitrogen). pcDNA-NVF contains a CMV promoter driving expression of the coding sequence encoding a nuclear localization signal (Pro-Lys-Lys-Lys-Arg-Lys-Val) from SV40 large T antigen, a herpes simplex virus VP16 activation domain (amino acids 413–490), and a Flag peptide (Asp-Tyr-Lys-Asp-Asp-Asp-Asp-Lys). All of the ZFP expression vectors were constructed by subcloning of the ZFP fragments into the *Kpn*I and *Bam*HI sites in pcDNA-NVF (see Fig. 5A). pEPOZFP−862c-NF plasmid is similar to EPOZFP−862c, except that the VP16 transactivation domain

was removed. The pBS579 construct, which was used as a negative control, encodes a nonspecific ZFP gene.

Cell Culture: Stable Inducible Cell Lines Expressing ZFPs, Luciferase Reporter Assays, Northern Blots, Taqman Analysis, ELISA, and Western Blots—Human embryonic kidney cells (HEK293) were grown in Dulbecco's modified Eagle's medium supplemented with 10% fetal calf serum. To generate stable inducible Tet-inducible EPOZFP cell lines, the coding region from the pEPOZFP−862 cDNA was subcloned into pcDNA4/TO (Invitrogen) using *Afl*III and *Hin*dIII restriction sites. The resulting pTO-EPOZFP−862 construct was transfected into the T-Rex-293™ (Invitrogen) cell line using LipofectAMINE (Life Technologies, Inc.). After 2 weeks of selection in medium containing Zeocin™ (Invitrogen), stable clones were isolated and analyzed for doxycycline (Dox)-dependent activation of ZFP expression.

The luciferase reporter constructs were generated by annealing two complementary oligonucleotides in an annealing buffer containing 50 mM NaCl, 10 mM Tris-HCl, 10 mM MgCl$_2$, 1 mM dithiothreitol. The oligo mixture was heated at 95 °C for 5 min and allowed to cool down slowly to room temperature. The annealed oligonucleotides containing three tandem repeats of the ZFP target sequences were inserted into the pGL3 promoter vector (Promega) between the *Mlu*I and *Bgl*II sites

---

A

FIG. 2. **The properties of EPOZFPs.**
A, schematic representation of the human EPO gene, showing key structural features. *Horizontal arrow,* start of transcription; *open rectangle,* coding region; *hatched boxes,* Alu elements; *black boxes,* targeted sequences, sites 1, 2, 3, and 4; *wavy lines,* CpG island. Abbreviations are as follows: *Ba, Bam*HI; *X, Xba*I; *Bg, Bgl*II; *Pst*I; *HRE,* hypoxic response element. Numbering is relative to the start site of transcription (+1). The targeted sites and the positions of the first nucleotide in the sequences is shown at the *bottom. B,* the protein gel shows all the purified EPOZFP, Sp1, and Zif268 proteins. The proteins were expressed as maltose-binding fusion proteins and purified as described (see "Experimental Procedures"). The *leftmost lane* contains size markers. *C,* gel-shift assays using the various EPOZFPs binding to their target sites. The name of each EPOZFP is indicated by the *number* in the *top left-hand corner* of each gel panel. Proteins are used to bind to their targets in 2-fold serial dilutions, with the highest protein concentration in *lane 2,* and the lowest concentration in *lane 16* from *left* to *right. Lane 1* is a control lane containing radiolabeled DNA alone. The equilibrium dissociation constants of each EPOZFP are indicated at the *top* of each panel.

-872
Site 1) GTGGGGGCTGGGTGCGGTGGCT

-544
Site 2) GGTGAGGAGTTGAGGTGGGG

-242
Site 3) CTCCCCTCCCGCGACCCA

-72
Site 4) CTCCCCCACCCCCACCCGC

B

130 KD
77 KD
43.3 KD   ← Purified ZFPs

C

- 826a GCG GTG GCT c Kd 6 nM   - 233 TGG GTC GCG g Kd 12 nM
- 862b GCG GTG GCT c Kd 9 nM   - 82 GTG GGG GAG a Kd 12 nM
- 862c GCG GTG GCT c Kd 2 nM   -72 GCG GGT GGG g Kd 22.5 nM
- 545a GGT GAG GAG t Kd 7.5 nM   Sp1 GGG GCG GGG Kd 40 nM
- 545b GGT GAG GAG t Kd 7 nM   Zif268 GCG TGG GCG t Kd 2 nM
-535 GAG GTG GGG a Kd 0.23 nM

upstream of the SV40 promoter. All constructs were confirmed by DNA sequencing.

Transient transfection was carried out using LipofectAMINE. Luciferase reporter assays were performed by co-transfection of ZFP effector DNA (50 ng), luciferase reporter DNA (900 ng), and pCMV-β-gal (100 ng, used as an internal control) into HEK293 cells seeded in six-well plates. Cell lysates were harvested 40 h after transfection, and the luciferase activities were measured by the Dual-Light luciferase and β-galactosidase reporter assay system (Tropix). To assay the activation of the endogenous chromosomal EPO gene, we made use of established procedures to carry out Northern analysis of EPO mRNA. Briefly, poly(A)[+] RNA was isolated from either mock-transfected or pcV-EPOZFP-862-transfected HEK293 cells using the Oligotex kit (Qiagen, Valencia, CA). 7 µg were resolved on a 2.4% agarose gel containing

2.4 M formaldehyde and blotted onto Nytran SuPerCharge membrane using 20× SSC. The membrane was hybridized at 65 °C for 1 h in Rapid-Hyb Buffer (Amersham Pharmacia Biotech) containing ^{32}P-labeled EPO cDNA probe. The same membrane was re-hybridized with a ^{32}P-labeled GAPDH DNA probe after stripping the EPO probe. The EPO cDNA construct, pcEPO was generated by inserting a human EPO cDNA fragment obtained by PCR amplification into the pcDNA3.1 vector (Invitrogen) at the *Xba*I and *Eco*RI sites. The clone was confirmed by sequencing. The pTBAHVP16 plasmid, which was used to generate riboprobes for detection of both human β-actin and ZFP genes, was generated by inserting the VP16 fragment from the pcDNANVF vector into the pTRI-β-actin-125-human vector (Ambion, Austin, TX). The pcDNA-NVF DNA was digested with *Xho*I, repaired with Klenow enzyme, and digested again with *Bam*HI. The TRI-β-actin vector was

digested with SmaI and BamHI.

For Taqman analysis of mRNA abundance, total cellular RNA from transfected HEK293 cells was isolated using the RNeasy kit (Qiagen, Valencia, CA). Real time PCR analysis (Taqman) was performed in a 96-well format on an ABI 7700 SDS machine (Perkin Elmer) and analyzed with SDS version 1.6.3 software. RNA samples (25 ng) were mixed with 0.3 μM each primer, 0.1 μM probe, 5.5 mM MgCl$_2$ and 0.3 mM each dNTP, 0.625 unit of AmpliTaq Gold RNA polymerase, 6.25 units of Multiscribe reverse transcriptase, and 5 units of RNase inhibitor in Taqman buffer A from Perkin Elmer. The reverse transcription was performed at 48 °C for 30 min. After denaturing at 95 °C for 10 min, PCR amplification reactions were conducted for 40 cycles at 95 °C for 15 s and at 60 °C for 1 min. The EPO primer and probe set (GACTGT-GTGCTCTGTGCACT, CTCTCAAAGTGCTGGGATTGCA, FAM-TGA-GCCACCGCACCCAGCCCCA-TAMRA) and the VP16 primer and probe set (CATGACGATTTCGATCTGGA, CTACTTGTCATCGTCGTC-CTTG, FAM-ATCGGTAAACATCTGCTCAAACTCGA-TAMRA) were used to measure the human EPO and ZFP expression levels, respectively. The GAPDH primer and probe set (CCTTTTGCAGACCACAGT-CCA, GCAGGGATGATGTTCTGGAGA, FAM-CACTGCCACCCAGAA-GACTGTGG-TAMRA) were used to monitor the internal control GAPDH mRNA. The abundance of expressed ZFPs was controlled for at both the RNA level as described above, but also by Western blotting. This analysis was performed by resolving 10 μg of whole cell lysates on a 10–20% Tris-HCl polyacrylamide gel containing SDS. Proteins were transferred onto a nitrocellulose membrane using 1× SDS, 20% Methanol, and then the filter was blocked using 5% nonfat dry milk for 1 h at room temperature. Blotting was done with anti-Flag M2 monoclonal antibody (Sigma) diluted 1:1000 in 5% (w/v) nonfat dry milk, 0.1% PBS-Tween) for 1 h at room temperature. Subsequently, an anti-mouse horseradish peroxidase conjugate (Amersham Pharmacia Biotech) was used at a 1:3000 dilution in 5% (w/v) nonfat dry milk, 0.1% PBS-Tween for 1 h at room temperature. All washes were done in 0.1% PBS-Tween. The protein bands were detected by the ECL system (Amersham Pharmacia Biotech).

Endogenous EPO expression was assayed either in response to transient transfection with ZFP effectors or in response to the induction of pEPOZFP–862a following stable transformation. Assays were performed at the indicated time after transfection. Either RNA was extracted as indicated above, or the culture medium was harvested for measurement of secreted EPO protein using the human EPO ELISA kit (R&D Systems, Minneapolis, MN).

Chromatin Analysis, Chromatin Immunoprecipitation, DNase I, and Micrococcal Nuclease Mapping—Chromatin immunoprecipitation was performed using a ChIP assay kit according to the instructions from the manufacturer (Upstate Biotechnology, Inc., Lake Placid, NY). Approximately 2 million cells were cross-linked with 1% formaldehyde for 10 min, washed with PBS, and lysed in lysis buffer. The cell lysate was sonicated on ice, resulting in a DNA fragment length of approximately 500 bp. After removing cell debris by centrifugation, immunoprecipitation was performed in ChIP dilution buffer overnight with 3 μg of VP16 1–21 antibody (Santa Cruz) or 10 μg of anti acetylated H3 antibody (Upstate Biotechnology). The antibodies were collected with Protein A-agarose and washed. The cross-linking was reversed by incubation at 65 °C for 4 h in the presence of 200 mM NaCl. The DNA was recovered by phenol/chloroform extraction and the abundance of particular sequences quantitated using real time PCR with the ABI 7700 sequence detector from Perkin Elmer/Applied Biosystems as described above. The standard Taqman reagents and the universal thermal cycling parameters were used (10 min at 95 °C, followed by 40 cycles of 15 s at 95 °C and 1 min at 60 °C). The primers had the following sequences: −1838F, TGGTACATCTGGTGCATTGTTG; 1838R, AAATAATAGA-CACACACAAGATAGTGAAAGC; −927F, ACACCACAGGTCAAATA-AACAGATG; −927R, ACTTTTAGTGCACAGAGCACACAGT; −363F, GGCTTCCAGACCCAGCTACATT; −363R, GGTCTTGGGCGGAGAC-TCA; +538F, GTGCCAGTGGAGAGGAAGCT; +538R, CAAACTTCA-ATCCTGGTGTGACA; +6839F, TGGGAGTACAGGCGTGAGC; +6839R, GGGAAAATGATGAAAGAGAAATCAA; hGAPDH-F, GACA-TCAAGAAGGTGGTGAAG; hGAPDH-R, AGCTTGACAAAGTGGTCG-TTG. The Taqman probes were labeled with FAM at the 5′ end and with TAMRA at the 3′ end. They had the following sequences: −1834P, AAG-GCGGTGACCCCCTGGAC; −927P, CATTGTGCAGGACACACATG-CACCTTG; −363P, CGGAACTCAGCAACCCAGGCATCT; +538P, TGGGCGCTGGAGCCACCACTTA; +6839P ACCGCGCCAGCCCGTG-TC; hGAPDH-P, CACTGAGCACCAGGTGGTCTCCT. For nuclease digestion, nuclei were isolated from HEK293 cells essentially as described (25). The nuclei were resuspended at 10,000/μl in digestion buffer. This suspension was aliquoted (100 μl) into tubes and digested with nuclease
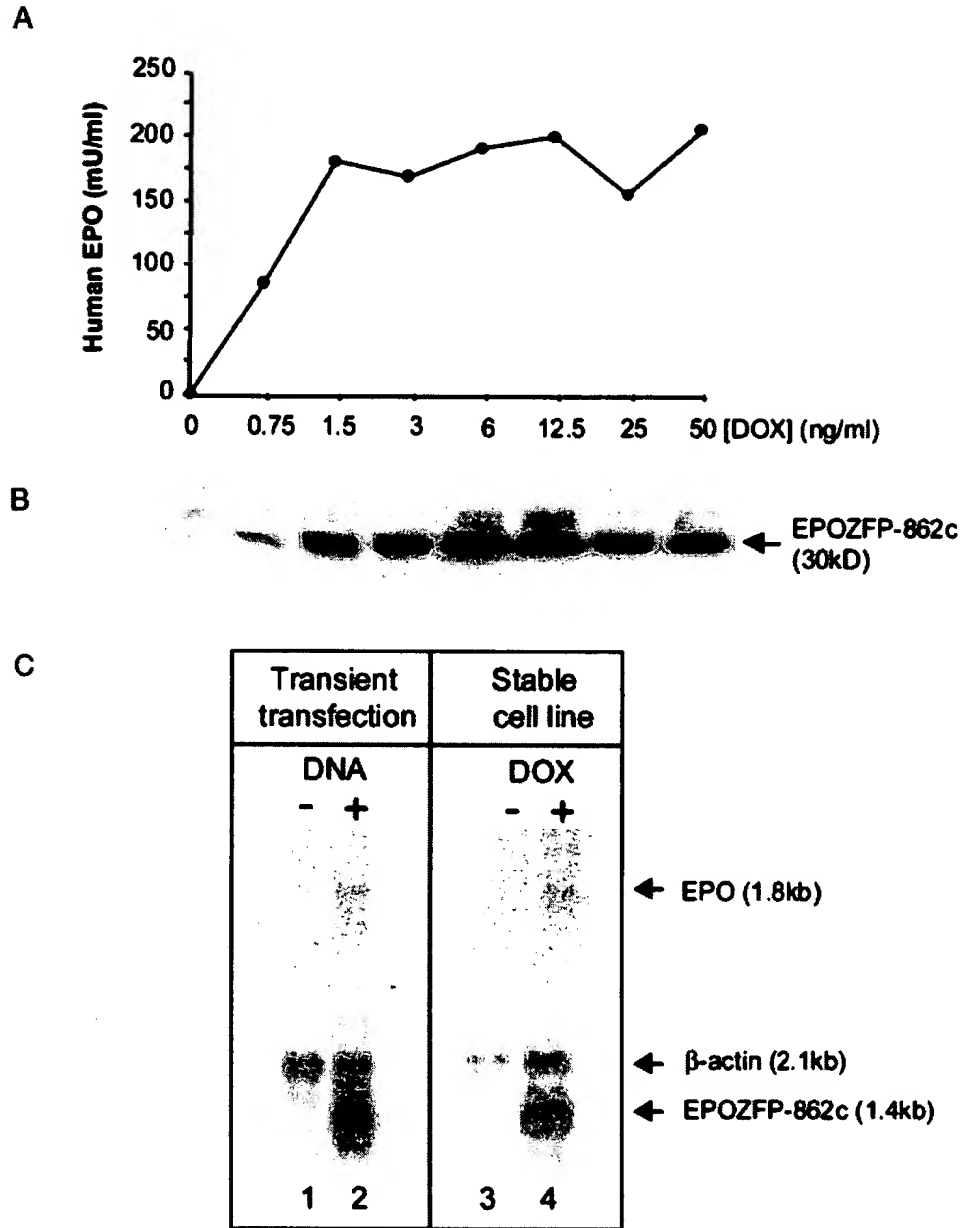
for 5 min at 22 °C. DNase I or micrococcal nuclease (Worthington) was added at 0, 5, 10, 20, or 40 units/ml for nuclei or 100-fold lower concentrations for naked DNA. The reaction was stopped by adding Qiagen buffer AL, followed by proteinase K treatment and purification (DNAeasy kit, Qiagen). The recovered DNA was digested to completion overnight at 37 °C with the indicated restriction endonuclease and then concentrated by ethanol precipitation. The entire sample is loaded onto an agarose gel of 1–2%, before electrophoresis and transfer to a Nytran membrane (Schleicher & Schuell). Indirect end labeling was used to detect the sites of nuclease cleavage. Hybridization was carried out in Rapid Hyb buffer (Amersham Pharmacia Biotech) using PCR-amplified genomic DNA fragments as indicated. The DNA probes were radiolabeled with [α-^{32}P]dCTP to a specific activity of 10^6 cpm/ng DNA. Hybridization and subsequent washings were performed at 65 °C. Membranes were visualized in the PhosphorImager.

RESULTS

Characterization of Synthetic ZFPs—We made use of existing information concerning the recognition of specific sequences by zinc finger domains to design 10 proteins that we predicted would recognize sequences in the 5′ flank of the human EPO gene. The strategy for assembly is illustrated in Fig. 1, and the details of design are summarized in Table I. The details of design and selection of zinc fingers capable of recognizing particular DNA sequences will be described in detail elsewhere.[2] The positions of the sequences within the human EPO gene that are targeted by our ZFP designs are illustrated in Fig. 2A. The ZFPs were designed to bind at four sites; site 1 and site 2 flank an Alu element. Alu elements are known to position nucleosomes (28, 29); we chose these flanking sites because we wished to avoid sites within the presumed position of stable histone-DNA interactions. Sites 3 and 4 were located −72 to −300 bp from the transcription start site (+1). We wished to introduce ZFPs here because they would be adjacent to a known region (−61 to −45 bp) important in the regulation of the human EPO gene (30). We expressed these diverse zinc finger proteins in recombinant form and purified them (Fig. 2B). In the nomenclature that we use to describe these proteins, each of which interacts with 9 bp of DNA, the number after the prefix EPOZFP delineates the position of the first nucleotide of the recognition sequence relative to the transcription start site (+1). Thus, EPOZFP–862 describes a zinc finger protein that binds to a 9-bp sequence that is positioned −862 bp to the 5′ of the transcription start site. Where there are multiple designs to particular sequence, this is indicated by, e.g., −862a, −862b, and −862c (see Table I). The recombinant proteins were used in gel retardation assays to quantitate their binding affinities for naked DNA (Fig. 2C). These results are tabulated in Table II. Our results indicate that we have designed a range of zinc finger DNA binding domains that exhibit a range of affinities for particular DNA sequences in the 5′ flank of the EPO gene. These affinities range from dissociation constants of 0.23 nM (EPOZFP–535) to greater than 20 nM (EPOZFP–72). We next wished to relate these proteins and

A

B

FIG. 3. **The transcriptional activation properties of the EPOZFPs.** *A*, luciferase reporter assays involved the co-transfection of the ZFP expression construct (50 ng) together with the respective luciferase reporter DNA (900 ng) (see "Experimental Procedures") and CMV β-gal as an internal control into HEK293 cells. After 40 h, cell lysates were harvested and the luciferase activity induced by each EPOZFP measured as indicated. The pcDNANVF and −862c-NF provide controls using proteins lacking the zinc fingers and VP16 activation domain, respectively. *B*, ELISA assays on endogenous EPO expression. EPO protein synthesis was assayed at 40 h after expression of the various EPOZFPs indicated as described (see "Experimental Procedures"). SBS 579 contains an expression vector for a nonspecific ZFP. *C*, quantitation of EPO mRNA by real time PCR (Taqman). EPO mRNA was assayed by real time PCR as described (see "Experimental Procedures") after expression of the various EPOZFPs for 40 h as described. SBS 579 contain an expression vector for a nonspecific ZFP. *D*, quantitation of the various EPOZFP mRNAs by real time PCR. The mRNA synthesized from the various transiently transfected EPOZFP expression constructs and their controls is quantitated. *E*, immunoblot of protein synthesized from the various transfected EPOZFPs and their controls.

C

D

E

A

B

EPOZFP-862c
(30kD)

C

Transient transfection	Stable cell line
DNA	DOX
− +	− +

← EPO (1.8kb)

← β-actin (2.1kb)
← EPOZFP-862c (1.4kb)

1 2   3 4
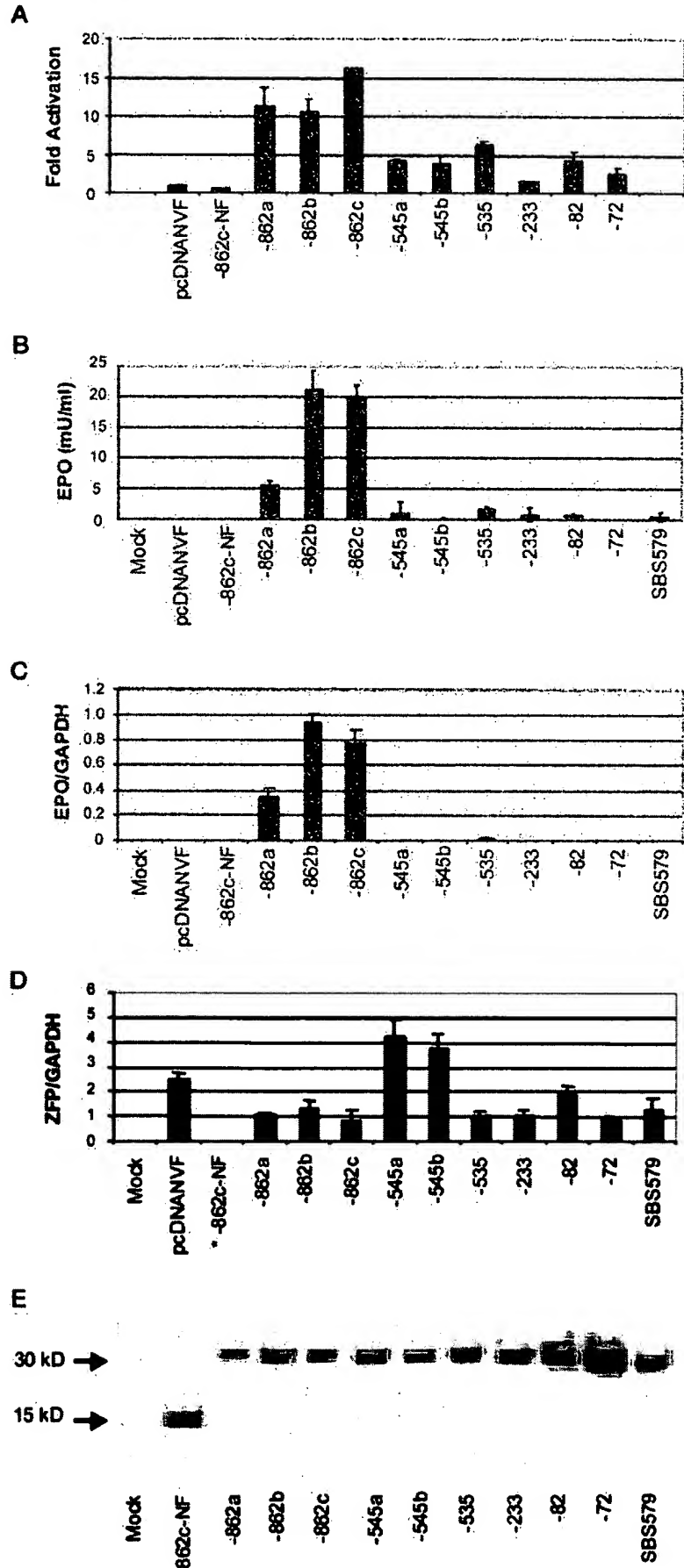
FIG. 4. **Inducible expression of the endogenous EPO gene in response to synthesis of EPOZFP−862.** *A*, EPO expression and Dox dose-response curve for stably transformed 293 cells containing copies of the EPOZFP−862c gene under control of a Tet-responsive full-length CMV promoter (see "Experimental Procedures"). Conditioned medium was harvested 48 h after the addition of Dox at the concentrations indicated and analyzed by an EPO ELISA kit (see "Experimental Procedures"). *B*, EPOZFP−862 immunoblot. Protein extracts from cells treated with the indicated Dox concentrations were analyzed by immunoblotting with the anti-Flag antibody. Extracts were prepared from cells 48 h after induction. *C*, Northern blot analysis of EPO mRNA induced by EPOZFP−862. EPO mRNA signals were shown for EPOZFP−862c-transfected 293 cells and for Dox-induced EPOZFP−862 cells (*lanes 2* and *4*, respectively). As a control untransfected (*lane 1*) and Dox-minus cells (*lane 3*) are also used to extract mRNA. The EPO probed membrane was stripped and rehybridized with a ^{32}P-labeled riboprobe containing antisense fragments that hybridize to ZFP mRNA as well as to the human β-actin gene that served as as a loading control.

their recognition of these diverse sequences to their capacity to activate transcription from the EPO promoter when fused to a luciferase reporter.

Transcriptional Regulation of the EPO Promoter Using ZFPs—Intensive analysis has defined the key cis-acting elements for regulation of the human EPO promoter. Erythropoietin is a protein hormone produced primarily in the kidneys and liver which controls the biogenesis of erythrocytes. Expression of the EPO gene is primarily controlled in a tissue-specific manner that is sensitive to oxygen tension. Hypoxia induces EPO gene expression at the transcriptional level through the action of a hypoxia response element, which interacts with

HIF-1, a heterodimer of the PAS-family transcription factor HIF-1α and ARNT, the aryl hydrocarbon receptor nuclear translocator (31). The hypoxia response element is located at the 3' flank of the EPO gene (31–33). A homodimer of HNF-4 also binds at this site (32, 33). The 5' flank of the EPO gene has also been determined to influence transcription; however, the only known regulatory elements that contribute to EPO gene activity within this DNA segment are located proximal to the start site of transcription (between −61 and −45 relative to the start at +1) (30). All ZFP transcription factors activate the luciferase reporter gene (Fig. 3A). These constructs contain three reiterations of the ZFP recognition site upstream of the
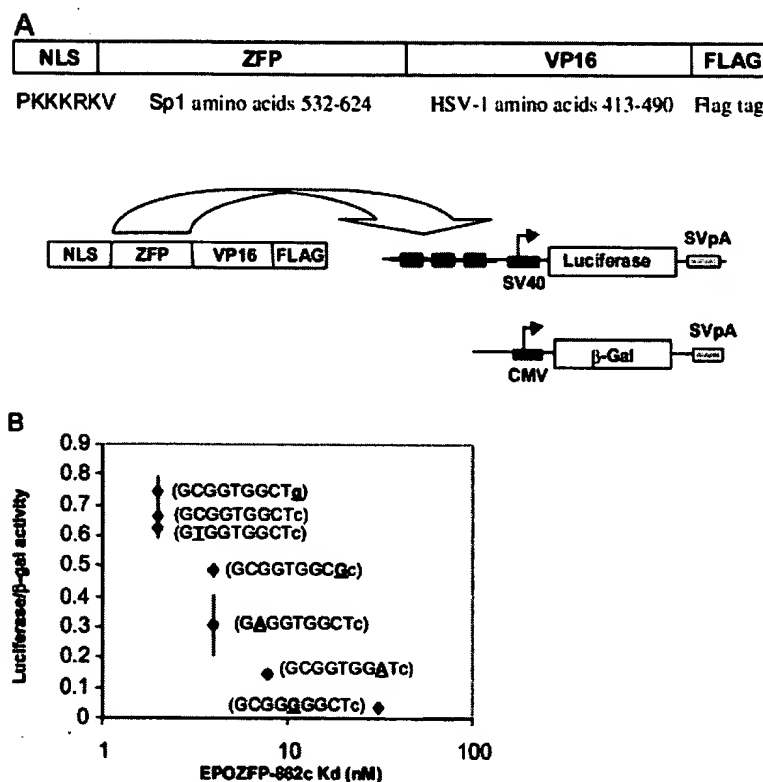
FIG. 5. **The relationship of DNA binding affinity to transcriptional activation for EPOZFP–862c on transiently transfected DNA.** *A*, schematic representation of the experiment. The organization of the EPOZFP–862 protein is shown. In this experiment the stably integrated EPOZFP–862c gene was induced by Dox in 293 cells. The expressed EPOZFP–862 protein binds to the transiently transfected luciferase reporter gene whose activity is dependent on three tandem copies of the EPOZFP–862 target sequence. The perfect EPOZFP–862 target sequence and mutant versions of this sequence to which EPOZFP–862 binds with varying affinity were inserted into the luciferase reporter construct and the capacity of EPOZFP–862 protein to activate these reporters quantitated relative to CMV-driven β-gal as a control. *B*, luciferase assays *versus* EPOZFP–862c. The individual reporter constructs as indicated were transfected into the T-Rex EPOZFP–862c stably transformed 293 cells. After 24 h of induction with Dox (0.05 μg/ml), the activities of the luciferase and internal control β-gal were measured. The normalized luciferase activities were graphed against the corresponding K_d values, which are represented on a log scale. Standard deviations are shown.

SV40 minimal promoter. Expression of a ZFP that lacks the VP16 activation domain does not activate luciferase (Fig. 3*A*, *NVF*). The range of activation varies between 2-fold (EPOZFP–233) and 16-fold (EPOZFP–862c). Surprisingly, in the data shown in Fig. 3*A* and in all subsequent repetitions of this experiment, there is no strong correlation in these transient assays between the capacity of a ZFP to activate transcription and the measured binding affinity (Table II). Both the strong (EPOZFP–535), K_d = 0.23 nM) and weak (EPOZFP–72, K_d = 22.5 nM) binders activate transcription with comparable efficiency. Although these results indicate that our basic design of ZFP transcription factors is robust, there are several variables to interpretation of these data. The newly synthesized ZFPs might have varying stability, or be deficient in entry into the nucleus, or might be engaged in non-productive protein-protein interactions with inhibitory factors. We have controlled for these possibilities in various ways. Western blotting demonstrates that all of the ZFPs accumulate to high levels in cells (see Fig. 3*E*) and the cells accumulate comparable levels of ZFP encoding mRNA (see Fig. 3*D*). In other experiments, we have established that the ZFPs accumulate uniformly in nuclei and that they retain identical capacities within nuclear extracts prepared from these cells to recognize that DNA sequences to which they bind *in vitro* (data not shown).

In order to further test the relationship between DNA binding affinity and the capacity of the ZFPs to activate the EPO gene by virtue of their binding at a particular site, we established an inducible cell line expressing the most effective activating ZFP in our transient expression assays, EPOZFP–862.

Our strategy was to transfect pTO-EPOZFP–862c into the T-Rex −292™ cell line (see "Experimental Procedures"), which stably expresses the Tet repressor and allows for the regulated expression of a gene of interest under the control of a Tet-responsive promoter when doxycycline is added to the culture medium. Twenty-one stable clones were isolated and analyzed for ZFP expression and erythropoietin expression in a Dox-dependent manner (Fig. 4, *A* and *B*). We used Northern blotting to confirm that the endogenous human EPO chromosomal locus was activated to synthesize a full-length poly(A)⁺ mRNA in response to either transient or stable expression of EPOZFP–862 (Fig. 4*C*).

We next investigated the activation of a luciferase reporter to which was fused at the same site relative to the SV40 minimal promoter three reiterations of the EPOZFP–862 recognition sequence and mutant forms of this sequence to which EPOZFP–862 has reduced binding affinity (Fig. 5*A*). Under these defined conditions, there is a strong correlation between the ZFP affinity for a particular sequence and the capacity to activate transcription (Fig. 5*B*). We suggest that, within one defined chromosomal or chromatin context, a particular ZFP will regulate transcription in a manner that largely reflects relative binding affinity for the cognate sequence. Transcriptional activation occurs most efficiently when the K_d is progressively reduced from 10 nM and is relatively inefficient when the K_d exceeds 30 nM (Fig. 5*B*). This contrasts with the lack of correlation between binding affinity and transcriptional response apparent when different ZFP binding sites relative to the transcription start site are used in luciferase reporter as-
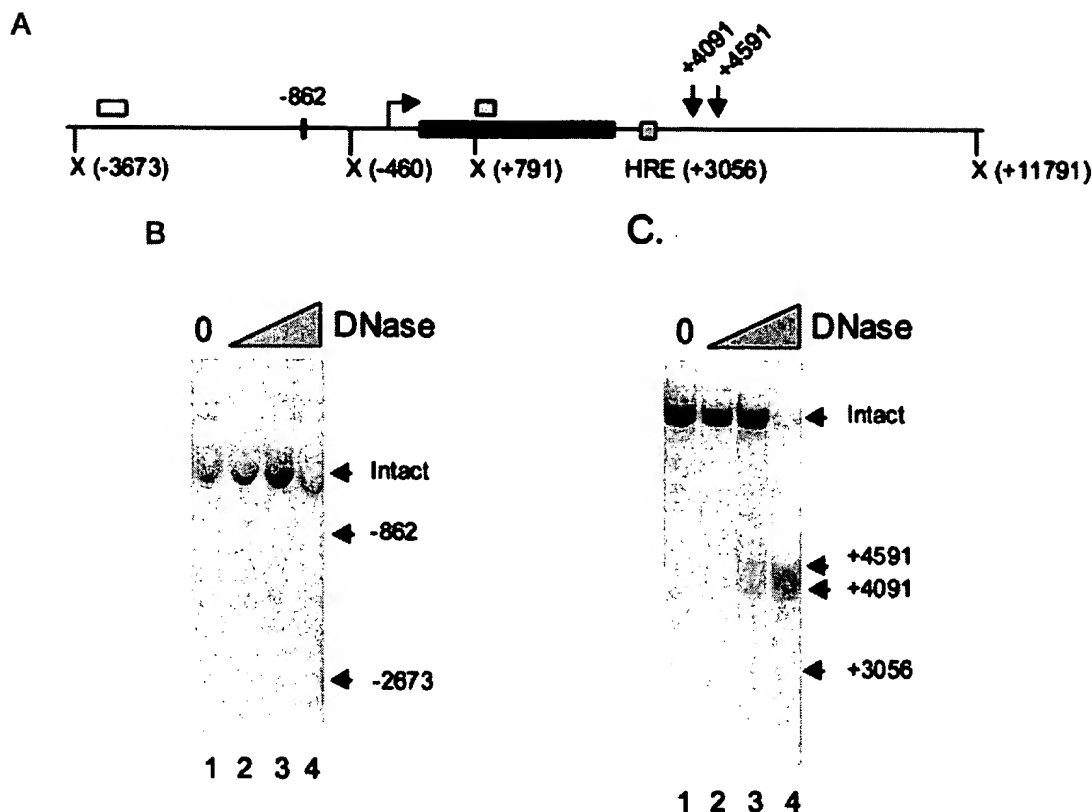
FIG. 6. **The promoter of the human EPO gene is not hypersensitive, but the 3'-flanking sequence is hypersensitive to DNase I cleavage.** *A*, a scheme showing restriction sites ($X = X$baI), probes (*hatched boxes*), coding region (*solid rectangle*), and hypoxia response element (*gray box*). *B*, nuclei were treated with DNase I (see "Experimental Procedures") at 0, 5, 10, or 20 units/ml (*lanes 1–4*), then digested with XbaI and probed with a* fragment abutting −3673. Positions of DNA sizes relative to the transcription start are shown. *C*, the *blot* shown in *panel B* was stripped of probe and rehybridized to detect DNase I-hypersensitive sites at the 3' distal region. The DNA fragment that anneals near the +791 XbaI site was used as a probe. Relative positions of DNase I-hypersensitive sites (+4591 and +4091) plus the position of the hypoxic response element are indicated.

says and in activation experiments on the endogenous chromosomal locus (Table II, Fig. 3, *A–C*).

We next compared the capacity of ZFPs that would recognize sequences present in the 5' flank of the EPO gene *in vitro* on naked DNA and *in vivo* on transiently transfected DNA, to activate the endogenous chromosomal locus. In Fig. 3 (*A–C*), we compare the capacity of ZFPs to function in the luciferase reporter assay with their capacity to activate the endogenous EPO gene as assayed both by quantitative real time PCR (Taqman) and by ELISA assays. We find that, in contrast to the pleiotropic activation of the transiently transfected reporter construct (Fig. 3*A*), activation of the endogenous chromosomal EPO promoter is found with those ZFPs targeted to one selected target in the promoter (Fig. 3, *B* and *C*). This is the binding site for EPOZFP−862. Three individual protein designs with varying affinity for DNA (EPOZFP−862a, -b, and -c) activate the endogenous chromosomal EPO gene at this site. All other ZFPs targeted elsewhere in the 5'-flanking sequences of the EPO gene are reduced in their capacity to activate transcription (Fig. 3*C*). These results indicate that there exist constraints on ZFP function on the endogenous chromosomal EPO gene.

Analysis of ZFP Access to the Chromatin Infrastructure— There are no documented regulatory elements in the 5' flank of the EPO gene beyond the immediately proximal promoter region between −61 and −45 (30). All other defined regulatory elements lie 3'. Thus, the capacity of three ZFPs targeted to the site 1 region (Fig. 2*A*) at −862 would appear to generate a novel cis-acting element *de novo*. In order to further test this idea, we

performed a DNase I hypersensitivity analysis of the promoter region. We did not detect preferred sites of cleavage in the vicinity of −862, nor were any sites detectable within 3 kilobase pairs between −460 and −3673 5' of the EPO transcription unit (Fig. 6, *A* and *B*). This lack of DNase I hypersensitivity might be anticipated because the promoter is normally silent in 293 cells (30–33). In contrast to the lack of DNase I hypersensitivity in the immediate vicinity of the quiescent EPO promoter, robust sites of DNase I hypersensitivity are found at the 3' flank of the previously documented hypoxia response element (Fig. 6, *A* and *C*). This result leads to the observation that the EPOZFP−862a, -b, and -c proteins are not gaining access through a preexisting DNase I-hypersensitive site in chromatin.

Our evidence for the EPOZFP−862a, -b, and -c proteins functioning at Site 1 (Figs. 2 and 3) led us to employ a more direct strategy to test our hypothesis that these ZFPs were gaining access to the chromatin infrastructure at this site. Chromatin immunoprecipitation is a powerful method to demonstrate selective enrichment of a particular regulatory protein at a particular site in chromatin (34). We chose to test for enrichment of the EPOZFP−862 protein both at site 1 and at a second site of perfect identity located at +6826 relative to the transcription start site. After cross-linking and immunoprecipitation using antibodies against VP16 (see "Experimental Procedures"), we made use of three primer pairs centered on 5'-flanking regions −1838, −927, −363 and two sets of primer pairs centered on sequences downstream from the start site of transcription at +538 and the other site of perfect identity

A

B

C
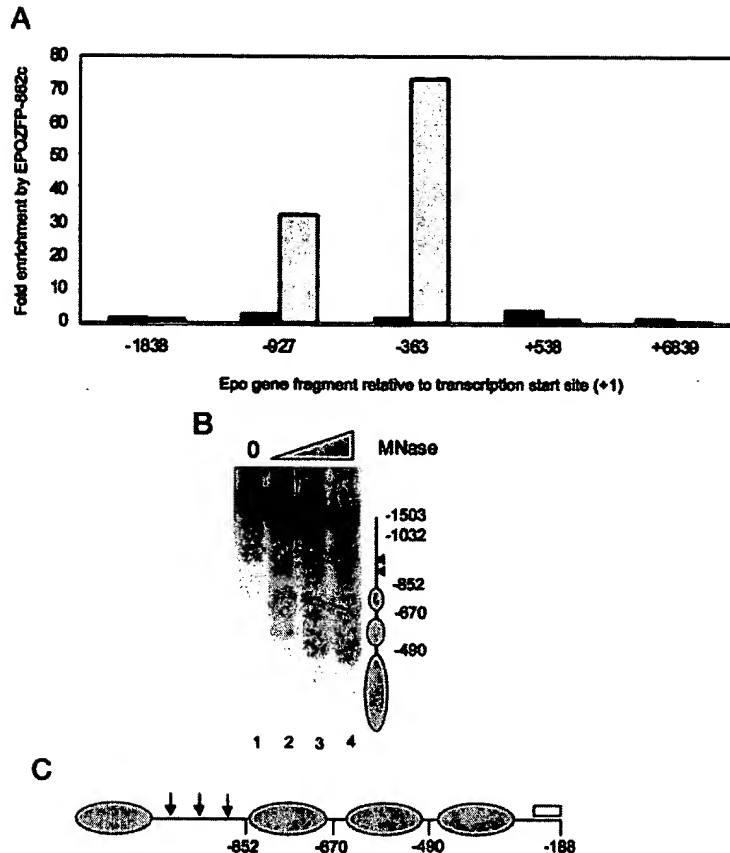
FIG. 7. **The EPOZFP–862c protein accumulates in chromatin.** *A*, 24 h after induction of EPOZFP–862c in the doxycycline-regulatable cell line, the *in vivo* binding of the EPOZFP–862c protein along the endogenous EPO locus was analyzed using chromatin immunoprecipitation using an antibody against the VP16 domain or EPOZFP–862c (see "Experimental Procedures"). Five primer pairs were used to scan the distribution of EPOZFP–862c along the EPO locus. A control nonspecific antibody was also used for immunoprecipitation. A primer pair contained within the human GAPDH gene was used to normalize signals. *B*, nuclei isolated from HEK293 cells were treated with micrococcal nuclease (*Mnase*), followed by deproteinization and subsequent digestion with *Pst*I. Nucleosomal ladders were visualized by indirect end labeling with a *Pst*I-*Hinc*II fragment (base pairs –188–469). The micrococcal nuclease concentrations were 0.5, 10, and 20 units/ml, respectively. Markers were run on the same gel to enable the accurate determination of fragment sizes. The interpretative scheme indicates the potential positions of nucleosomes and their linkers. *C*, a scheme representing the potential translational positioning of nucleosomes in the human erythropoietin gene. *Arrows* represent the sites of substantial access for micrococcal nuclease, *ovals* represent nucleosomes, and the *open box* represents the *Pst*I-*Hinc*II probe. *Numbers* show the approximate positions of linker regions relative to the transcription start site.

+6839. The abundance of these DNA sequences was quantitated relative to a GAPDH internal control. Our results show a 30–70-fold enrichment between the −927 and −363 sites for the EPOZFP–862 protein (Fig. 7A). This distribution might be expected due to our use of DNA fragments of 500 bp in size in our chromatin immunoprecipitation assays. Both the −927 and −363 fragments would contain the −862 site within this size distribution. An additional important control is the loss of recovery of DNA fragments at both the 5′ (−1838) and 3′ (+538) regions flanking the −862 site (Fig. 7A). Finally, it is noteworthy that an identical sequence, GCGGTGGCT, for recognition by EPOZFP–862 positioned at +6839 is not recovered at all in this experiment. (Fig. 7A). We conclude that parameters other than DNA sequence *per se* determine the access of the EPOZFP–862 protein to the cognate sequence.

In order to better understand the access of EPOZFP–862 protein to the endogenous chromosomal EPO locus, we made use of micrococcal nuclease digestion of chromatin. This enzyme is considerably smaller than DNase I and gains efficient access to the linker DNA between nucleosomes (35). Sequence analysis of the 5′ flank of the EPO gene indicates the presence of Alu elements, which are known to position nucleosomes (28, 29). The EPOZFP–862 site is at the 5′ of the Alu element (Fig. 7A), which we would predict would lie in linker sequence adja-

cent to the nucleosome core. To test this hypothesis, we digested chromatin with micrococcal nuclease and then used indirect end labeling to determine the positions of nucleosomes. We find that nucleosomes are positioned such that linker DNA is accessible at −490 and −670 with a major region of micrococcal nuclease sensitivity beginning at −852. Thus, a domain of micrococcal nuclease sensitivity corresponds to a site of responsiveness to EPOZFP–862.

As a test of the capacity of the EPOZFP–862 protein to initiate events leading to chromatin remodeling, we examined the chromatin structure of the endogenous EPO gene in the cell line that induced expression of EPOZFP–862 in response to doxycycline. In the absence of EPOZFP–862 expression, there is no significant expression of the endogenous EPO gene (Figs. 3 and 4) and there is no DNase I hypersensitivity over the promoter (Fig. 6, *A* and *B*). In the presence of doxycycline, the endogenous EPO locus is transcriptionally activated (Figs. 3 and 4) and a DNase I-hypersensitive site appears over the promoter (Fig. 8, *A* and *B, lanes 1* and *2*). In the absence of doxycycline, no DNase I-hypersensitive site appears (Fig. 8, *A* and *B, lanes 3* and *4*). These results confirm the capacity of the synthetic transcriptional regulators to remodel chromatin in a targeted manner.

A

B
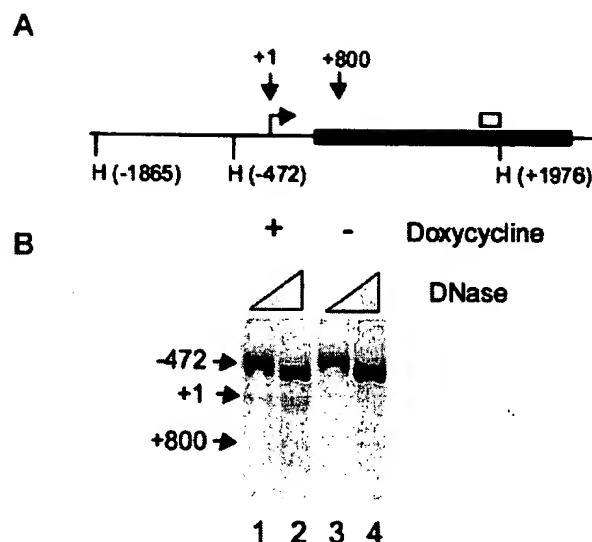
FIG. 8. **An inducible DNase I-hypersensitive site in the EPO promoter dependent on expression of EPOZFP−862.** *A*, scheme of the EPO gene around the transcription start site (+1). The gene is indicated by the *solid rectangle* and the probe by the *open box*. H indicates *Hinc*II cleavage sites. *B*, nuclei from cells treated with 5 ng/ml Dox (*lanes 1* and *2*) or untreated cells (*lanes 3* and *4*) were isolated and treated with 10 or 20 units/ml DNase I, respectively. The DNA was isolated and digested with *Hinc*II before probing with a DNA fragment that anneals near the *Hinc*II site at position +1976.

DISCUSSION

The primary conclusion from these experiments is that the activity of synthetic zinc finger transcription factors at an endogenous chromosomal locus (Figs. 3 (*B* and *C*) and 4) differs significantly from the determinants of protein binding to naked DNA (Fig. 2 and Table II) and from the capacity of these diverse proteins to activate transiently transfected templates (Figs. 3*A* and 5). Although there is little difficulty in activating transcription from transiently transfected templates (Fig. 3*A*), there are constraints in gaining access to sites within endogenous chromosomes in order to regulate expression (Figs. 3 (*B* and *C*) and 6–8). These observations are consistent with earlier work on the mouse mammary tumor virus promoter in which the access of the transcriptional regulators NF1 and Oct 1 is dependent on the nature of the chromatin infrastructure (36–38). The prior assembly of nucleosomes on the NF1 and Oct 1 binding sites precludes their access to the MMTV promoter in chromatin (36, 37). Chromatin remodeling events dependent on the glucocorticoid receptor are necessary to allow NF1 and Oct 1 to bind and function in transcriptional activation (38). Our observations that a ZFP binding site lies in an accessible linker region between nucleosomes and that this facilitates stable association with chromatin is also consistent with earlier work on the natural zinc finger protein TFIIIA (14–26).

Earlier experiments have demonstrated the capacity of designer zinc finger proteins to regulate transcription on transiently transfected templates (9–13). These templates are inefficiently assembled into chromatin if at all (39). For the MMTV promoter, the chromatin assembled on transiently transfected templates poses no measurable impediment to the association of NF1 and Oct 1 (36). In contrast, chromatin assembled on replicating episomes or within endogenous chromosomes poses a much severe impediment to transcription factor binding (36). In two instances, successful regulation of transcription by ZFP transcription factors within a chromosomal locus has been described (9, 13). These were the regulation of

the fusion oncogene for BCR-ABL by the DNA binding domain of a three finger zinc finger protein lacking any other regulatory domains (9), and the regulation of the erbB-2 locus by ZFPs to which were fused both activation and repression domains (13). The ZFP that functioned on the BCR-ABL oncogene has a very weak binding affinity for DNA, yet this protein was targeted to a randomly integrated cDNA construct representing the chromosomal breakpoint where the two genes were fused (9). These two structural features may very well represent particularly open regions of chromosomal structure. The ZFPs that regulate the erbB-2 chromosomal locus have much higher affinities for DNA (K_d = <1 nM) and are targeted to 5'-untranslated region of the erbB-2 oncogene (13). There is no reason to anticipate that such a region of chromatin would be more accessible to regulatory factors than other regions, and in fact we have tested several ZFPs that recognize the 5'-untranslated region of the EPO gene that do not activate transcription in our system. We predict that the ZFPs that regulate the endogenous erbB-2 locus do so by binding to an accessible linker DNA in chromatin. Future experiments will test this possibility.

We demonstrate that the EPOZFP−862 is highly enriched in chromatin in the vicinity of the designated recognition site in chromatin and that other proteins that selectively bind this site show comparable transcriptional regulatory effects (Figs. 3 and 7). There are no known transcriptional regulatory elements that normally contribute to EPO gene expression at this site (30–34). In fact, this region of the EPO gene is refractory to DNase I cleavage consistent with the lack of regulatory DNA (Figs. 6 and 8). Thus the targeting of EPOZFP−862 to a linker region flanking a nucleosome positioned on an Alu element generates a novel cis-acting element (Figs. 3 and 7).

These observations suggest an improved strategy for dissecting the requirements for eukaryotic gene control. First, it is important to determine the underlying chromatin infrastructure and identify linker DNA segments between positioned nucleosomes. Second, it should be possible to design ZFPs that will recognize these accessible sequences such that they bind stably in chromatin (Figs. 7 and 8). Third, it would then be possible to systematically recruit a variety of transcriptional activation or repression domains to that particular site in order to remodel chromatin and regulate transcription. In this way, it should be possible to manipulate human genes in their endogenous chromosomal context and more effectively design ZFPs with therapeutic potential.

REFERENCES

1. Desjarais, J. R., and Berg, J. M. (1992) *Proteins Struct. Funct. Genet.* **12**, 101–104
2. Desjarais, J. R., and Berg, J. M. (1993) *Proc. Natl. Acad. Sci. U. S. A.* **90**, 2256–2260
3. Rebar, E. J., and Pabo, C. O. (1994) *Science* **263**, 671–673
4. Jamieson, A. C., Kim, S.-H., and Wells, J. A. (1994) *Biochemistry* **33**, 5689–5695
5. Choo, Y., and Klug, A. (1994) *Proc. Natl. Acad. Sci. U. S. A.* **91**, 11163–11167
6. Wu, H., Yang, W.-P., and Barbas, C. F., III (1995) *Proc. Natl. Acad. Sci. U. S. A.* **92**, 344–348
7. Jamieson, A. C., Wang, H., and Kim, S.-H. (1996) *Proc. Natl. Acad. Sci. U. S. A.* **93**, 12834–12839
8. Greisman, H. A., and Pabo, C. O. (1997) *Science* **275**, 657–661
9. Choo, Y., Sanchez-Garcia, I., and Klug, A. (1994) *Nature* **372**, 642–645
10. Kim, J.-S., and Pabo, C. O. (1997) *J. Biol. Chem.* **272**, 29795–29800
11. Kim, J.-M., Kim, J., Cepek, K. L., Sharp, P. A., and Pabo, C. O. (1997) *Proc. Natl. Acad. Sci. U. S. A.* **94**, 3616–3620
12. Beerli, R. R., Segal, D. J., Dreier, B., and Barbas, C. F., III (1998) *Proc. Natl. Acad. Sci. U. S. A.* **95**, 14628–14633
13. Beerli, R. R., Dreier, B., and Barbas, C. F., III (2000) *Proc. Natl. Acad. Sci. U. S. A.* **97**, 1495–1500
14. Wolffe, A. P., and Hayes, J. J. (1999) *Nucleic Acids Res.* **27**, 711–720

15. Gottesfeld, J., and Bloomer, L. S. (1982) *Cell* **28**, 781–791
16. Rhodes, D. (1985) *EMBO J.* **4**, 3473–3482
17. Tremethick, D., Zucker, D., and Worcel, A. (1990) *J. Biol. Chem.* **265**, 5014–5023
18. Ura, K., Hayes, J. J., and Wolffe, A. P. (1995) *EMBO J.* **14**, 3752–3765
19. Panetta, G., Buttinelli, M., Flaus, A., Richmond, T. J., and Rhodes D. (1998) *J. Mol. Biol.* **282**, 683–697
20. Hayes J. J., and Wolffe A. P. (1992) *Proc. Natl. Acad. Sci. U. S. A.* **89**, 1229–1233
21. Tse, C., Fletcher, T. M., and Hansen, J. C. (1998) *Proc. Natl. Acad. Sci. U. S. A.* **95**, 12169–12173
22. Lee, D. Y., Hayes, J. J., Pruss, D., and Wolffe, A. P. (1993) *Cell* **72**, 73–84
23. Vitolo, J. M., Thiriet, C., and Hayes, J. J., (2000) *Mol. Cell. Biol.* **20**, 2167–2175
24. Bouvet, P., Dimitrov, S., and Wolffe, A. P. (1994) *Genes Dev.* **8**, 1147–1159
25. Chipev, C. C., and Wolffe, A. P. (1992) *Mol. Cell. Biol.* **12**, 45–55
26. Sera, T., and Wolffe, A. P. (1998) *Mol. Cell. Biol.* **18**, 3668–3680
27. Triezenberg, S. J., Kingsbury, R. C., and McKnight, S. L. (1988) *Genes Dev.* **2**, 718–729
28. Englander, E. W., Wolffe, A. P., and Howard, B. H. (1993) *J. Biol. Chem.* **268**, 19565–19573
29. Englander, E. W., and Howard, B. H. (1995) *J. Biol. Chem.* **270**, 10091–10096
30. Gupta, M., and Goldwasser, E. (1995) *Nucleic Acids Res.* **24**, 4768–4774
31. Chan, W. K., Yao. G., Gu, Y.-Z., and Bradfield, C. A., (1999) *J. Biol. Chem.* **274**, 12115–12123
32. Lee, H. J., Young, W.-J., Shih, C. C.-Y., and Chang, C. (1997) *J. Biol. Chem.* **271**, 10405–10412
33. Hu, B., Wright, E., Campbell, L., and Blanchard, K. L. (1997) *Mol. Cell. Biol.* **17**, 851–856
34. Crane-Robinson, C., and Wolffe A. P. (1998) *Trends Genet.* **14**, 477–480
35. Drew, H. R. (1984) *J. Mol. Biol.* **176**, 535–557
36. Archer, T. K., Lefebvre, P., Wolford, R. G., and Hager, G. L. (1992) *Science* **255**, 1573–1576
37. Archer, T. K., Cordingley, M. G., Wolford, R. G., and Hager, G. L. (1991) *Mol. Cell. Biol.* **11**, 688–698
38. Fryer, C. J., and Archer, T. K. (1998) *Nature* **393**, 88–91
39. Reeves, R., Gorman, C. M., and Howard, B. H. (1985) *Nucleic Acids Res.* **13**, 3599–3615